

Supporting Information for :

**Polydopamine-functionalized Selenium Nanoparticles as an efficient
Photoresponsive Antibacterial Platform**

**Meng Sun,^{a,b} Ping Gao,^a Bao Wang,^a Xiangyang Li,^a Donghan Shao,^a Yan Xu,^a Leijiao Li,
^{*a,b} Yunhui Li, ^{*a,b} Jianwei Zhu,^b Wenliang Li ^{a,c} and Yingxue Xue ^{*c}**

^a School of Chemistry and Environmental Engineering, Changchun University of Science and Technology, Changchun, 130022, China.

^b Zhongshan Institute of Changchun University of Science and Technology, Zhongshan, 528437, China.

^c Jilin Medical University, Jilin, 132013, China.

1. Materials

Sodium selenite (Na_2SeO_3 95%) was purchased from Sigma-Aldrich. Polyvinylpyrrolidone (PVP), hydroxylamine (NH_2OH), and dopamine hydrochloride ($\text{C}_8\text{H}_{11}\text{NO}_2\text{-HCl}$ 98%) were purchased from Aladdin. Glutathione (GSH 98%) was obtained from Meryer. Indocyanine green (ICG 94%) was purchased from Meilunbio. 1,3-Diphenylisobenzofuran (DPBF 97%) was obtained from Mackin. DMEM medium (high sugar), EDTA-trypsin digest (0.25%), and fetal bovine serum (FBS) were purchased from Biological Industries. All chemical reagents were used as received.

2. Experimental Section

2.1 Synthesis of Se NPs and Se@PDA NPs

The Se@PDA samples were characterized by DLS, and UV-vis.

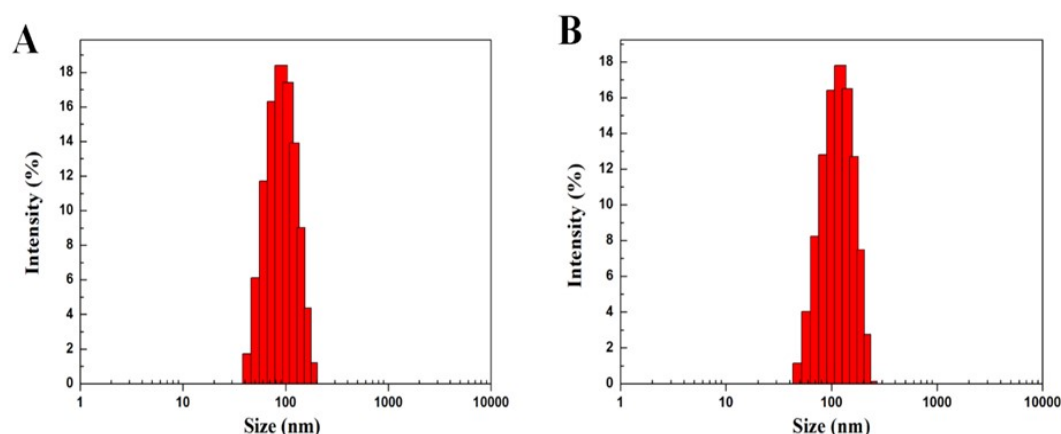


Fig. S1. Size distribution of Se NPs and Se@PDA samples in water. A) DLS data graph of Se NPs in aqueous solution. B) DLS data graph of Se@PDA in aqueous solution.

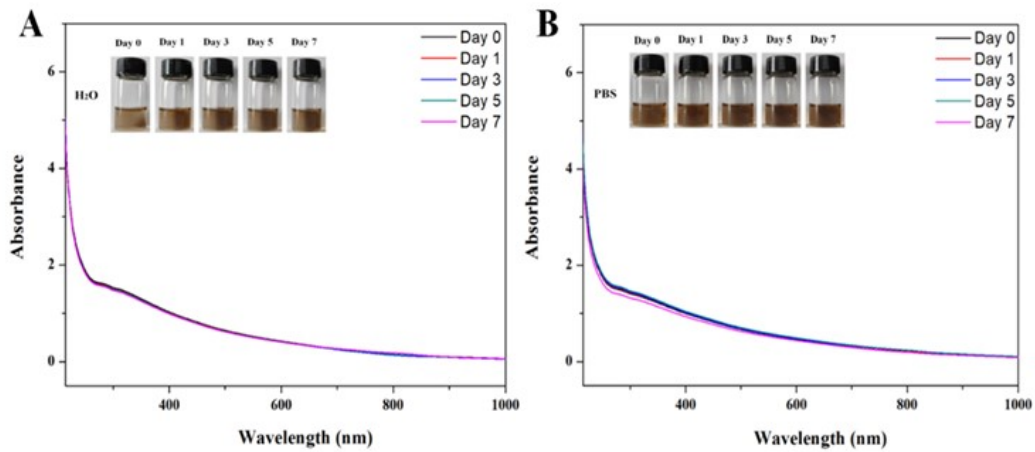


Fig. S2. The stability of Se@PDA. A) absorbance curve of the given number of days Se@PDA dispersed in water. B) The absorbance curve of Se@PDA dispersed in PBS on specified days.

2.2 Indocyanine green conjugation

Calculation of ICG load rate and Zeta potential of Se, Se@PDA, and Se@PDA-ICG in the illustration.

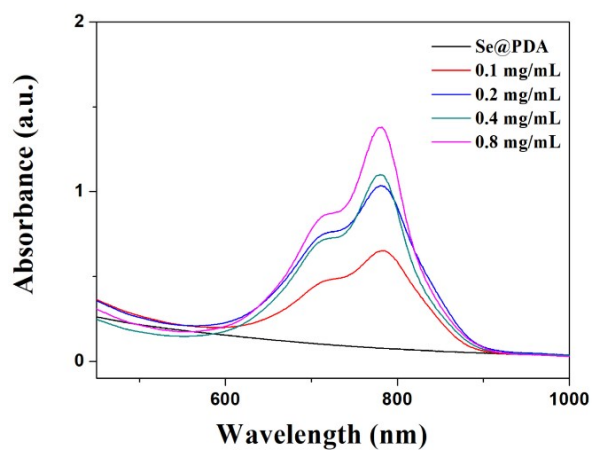


Fig. S3. UV-vis absorption spectra of Se@PDA incubated with different concentrations of ICG.

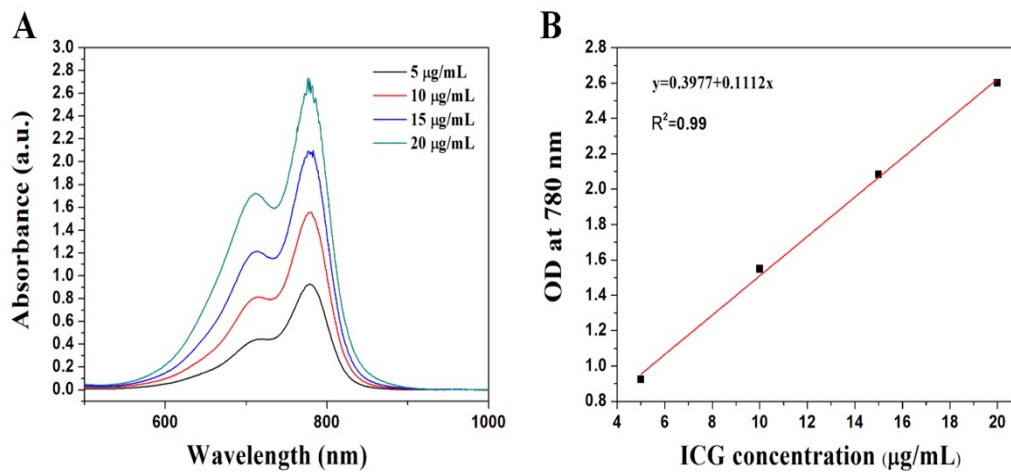


Fig. S4. Standard curve data for ICG A) UV absorption spectra of different concentrations of ICG. B) Standard curve of ICG solution.

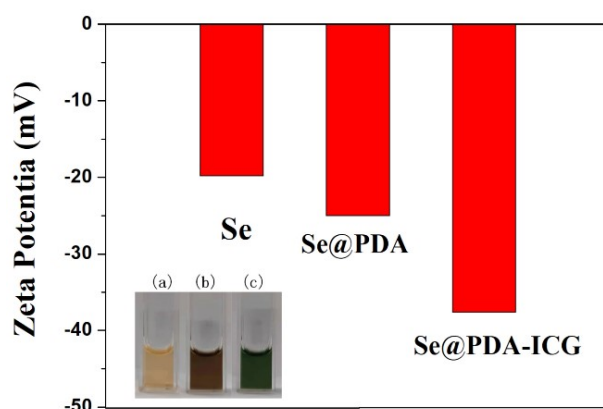


Fig. S5. Zeta potentials of Se, Se@PDA, and Se@PDA-ICG, in the illustration (a), (b), and (c) are physical images of aqueous solutions of Se, Se@PDA, and Se@PDA-ICG.

2.3 Singlet oxygen determination of Se@PDA-ICG

Testing the effect of Se@PDA-ICG to produce $^1\text{O}_2$ using a DPBF fluorescent probe.¹ Specifically, DPBF/DMSO (1.5 mg/mL) and Se@PDA-ICG (200 $\mu\text{g}/\text{mL}$) solutions were prepared separately, 20 μL of the DPBF solution was mixed with 2 mL of each component sample. Then the mixed solutions were irradiated using an 808 nm NIR laser (1 W/cm^2) and the samples were subjected to UV-vis detection at 2 min intervals to compare the DPBF absorption intensity at 417 nm.

2.4 Bactericidal effect *in vitro*

E. coli and *S. aureus* were used to evaluate the *in vitro* bactericidal effect of Se@PDA-ICG.

$$\text{Relative bacterial viability (\%)} = \frac{N_{\text{experiment}}}{N_{\text{control}}} \times 100\%$$

where, $N_{\text{experiment}}$ is the number of colonies in the experimental group, and N_{control} is the number of colonies formed in the PBS group.

2.5 Morphological study

For morphological characterisation of bacteria, bacterial suspensions from the PBS and Se@PDA-ICG treatment groups were fixed with fixative for 12 h after assessment of antimicrobial properties. They were then dehydrated with an ethanol gradient, dried, gold sprayed, and used for SEM observation.

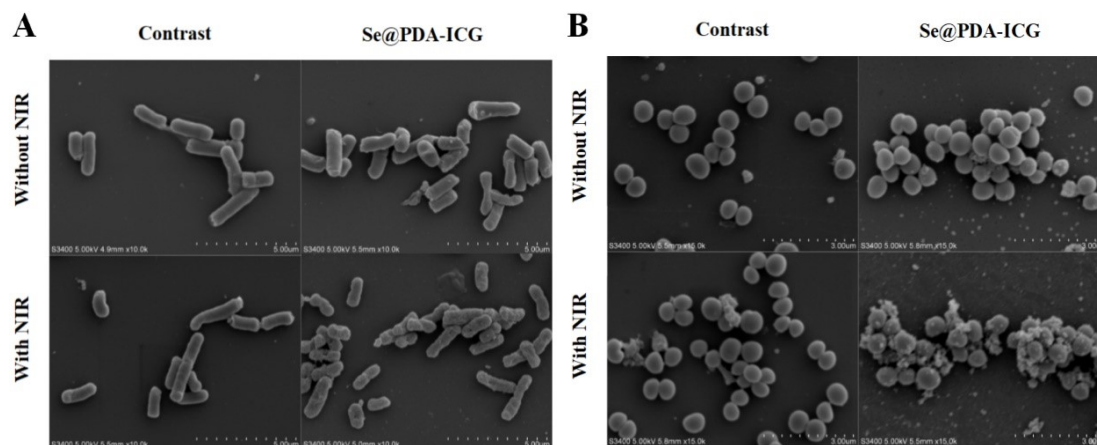


Fig. S6. Morphological changes of *E. coli* and *S. aureus* after incubated with Se@PDA-ICG (125 $\mu\text{g/mL}$). A) SEM images of *E. coli* after 808 nm laser irradiation were processed at Se@PDA-ICG. B) SEM images of *S. aureus* after 808 nm laser irradiation were processed at Se@PDA-ICG.

2.6 Hemolysis assay

A haemolysis assay was performed to assess *in vitro* biocompatibility. 1 mL of mouse blood was taken and centrifuged to obtain red blood cells (RBC) and washed with 5 mL PBS 5 times. After washing, the RBC were re-suspended with 10 mL PBS. RBC (0.2 mL) and suspension (0.8 mL) solution were uniformly mixed and incubated for 4 h, in which PBS and water were a negative and positive control group, and each concentration of Se@PDA-ICG solution was the experimental group. The suspension was centrifuged at 12000 rpm for 5 minutes to measure the absorbance of the supernatant. Finally, the hemolysis rate was calculated.²

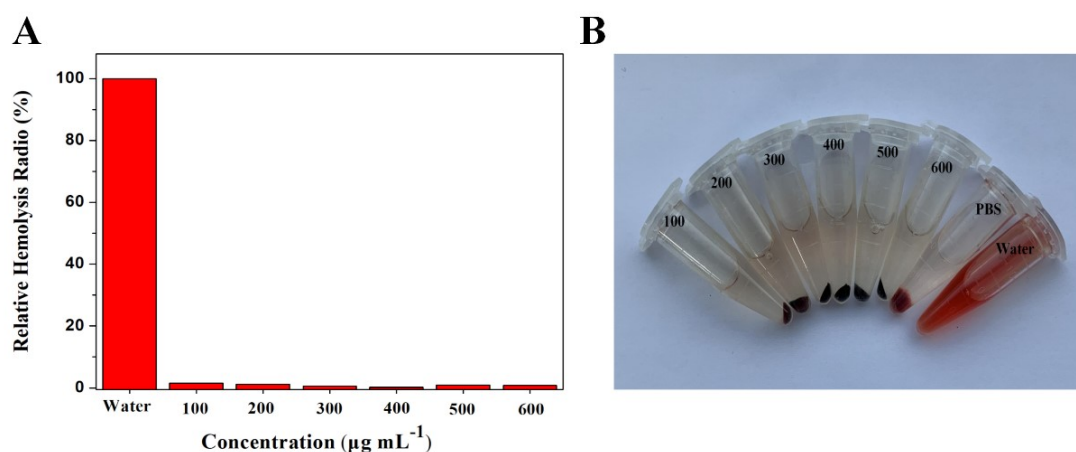


Fig. S7 Hemolysis test of Se@PDA-ICG. A) Data graphs of hemolysis percentage at different concentrations of Se@PDA-ICG. B) physical images of hemolysis percentage at different concentrations of Se@PDA-ICG.

2.7 Cytotoxicity study

Cytotoxicity data of Se@PDA-ICG materials.

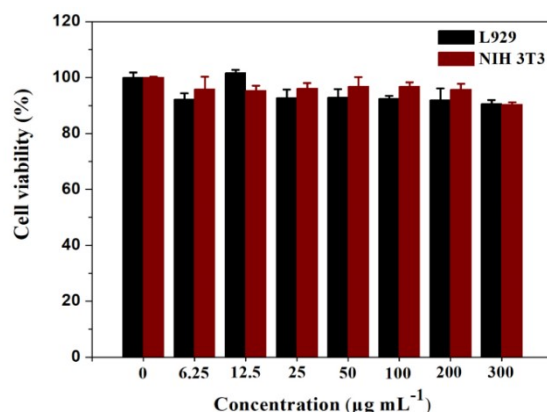


Fig. S8 MTT test results of L929 and NIH 3T3 fibroblasts at different concentrations of Se@PDA-ICG.

2.8 Biocompatibility test

The *in vivo* biocompatibility of the nano platform was evaluated by a mouse blood test. Healthy mice were randomly divided into Se@PDA-ICG experimental group and the PBS control group. Se@PDA-ICG solution (300 µg/mL) and PBS solution were injected into the two groups of mice through the tail vein (100 µL). The blood and serum of the mice were taken for biochemical analysis after the 7th day.

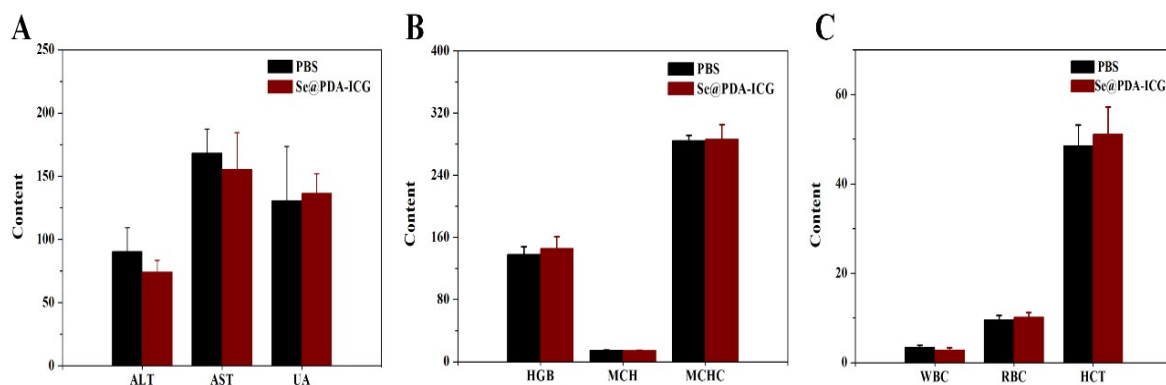


Fig. S9 Blood routine test data of mice 7 days after injection. A) Data of ALT, AST, and UA. B) Data of HGB, MCH and MCHC. C) Data of WBC, RBC, and HCT.

2.9 Bactericidal Effect *in vivo*

Calculation of Relative wound area in mice model.

$$\text{Relative wound area} = \frac{A_{\text{unhealed}}}{A_{\text{Original}}} \times 100\%$$

where, A_{unhealed} refers to the area of the unhealed wound area, and A_{Original} indicates the original wound area.

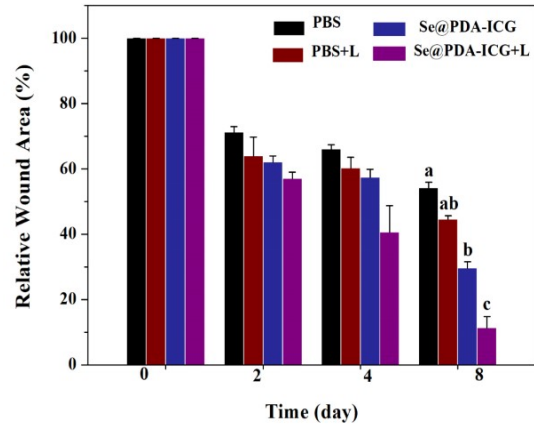


Fig. S10 Data chart of relative wound surface of mice in different treatment groups after 8 days of treatment ($p < 0.05$, $n = 3$).

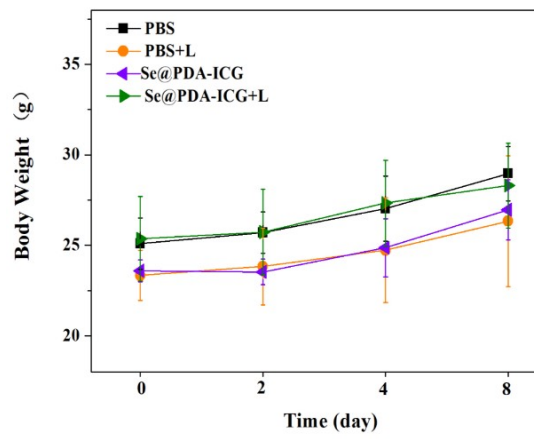


Fig. S11 Data were recorded on the body weight of each group of mice.

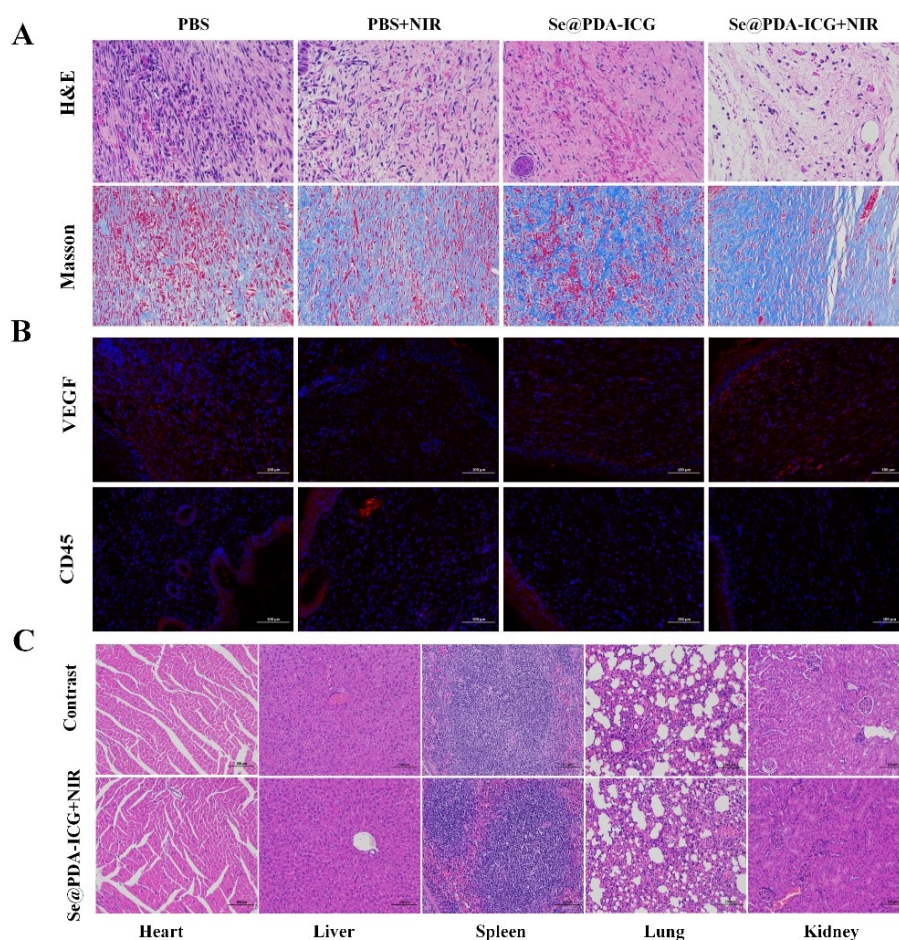


Fig. S12 Analysis of pathological sections on the 8th day of wound healing. A) Representative images of H&E and Masson staining of wounds in each group. B) Representative images of VEGF (VEGF fluorescence is red) and CD45 (CD45 fluorescence is red) immunofluorescence staining in wounds of each group. C) Representative images of H&E staining of major organs of mice in each group.

Notes and references

1. B. Li, C.X. Li, B.G. Xing, P.P. Yang, L. Jun, *J. Mater. Chem. B*, 2016, **4**, 4884-4894.
2. Y.N. Liu, Z.R. Guo, F. Li, Y.Q. Xiao, Y.L. Zhang, T. Bu, P. Jia, T.T. Zhe, L. Wang, *ACS Applied Materials & Interfaces*, 2019, **11**, 31649-31660.